Thermal quenching and retrapping effects in the photoluminescence of $In_yGa_{1-y}As/GaAs/Al_xGa_{1-x}As$ multiple-quantum-well structures

M. Vening* and D. J. Dunstan
Department of Physics, University of Surrey, Guildford, Surrey GU2 5XH, England

K. P. Homewood
Department of Electronic and Electrical Engineering, University of Surrey, Guildford, Surrey GU2 5XH, England
(Received 12 August 1992)

Multiple-quantum-well structures show thermally activated quenching of the photoluminescence. There are also small changes in photoluminescence intensity as carriers emitted from one well are retrapped in another. We present a coupled-well rate-equation theory which successfully models these changes in intensity in $In_yGa_{1-y}As/GaAs$ and $In_yGa_{1-y}As/GaAs/Al_xGa_{1-x}As$ structures. In both structures, the dominant nonradiative carrier loss from the wells is due to thermal excitation to the barriers; retrapping in the wells can be observed and is included in the model. In contrast, in $In_yGa_{1-y}As/Al_xGa_{1-x}As$ quantum wells, a defect-related nonradiative mechanism dominates even with an Al content in the $Al_xGa_{1-x}As$ of only 5%.

I. INTRODUCTION

Semiconductor strained-layer quantum wells are now finding applications in advanced optoelectronic devices such as strained-layer laser diodes.[1] These devices generally operate at room temperature or above, where thermal detrapping of carriers from the quantum wells to the barrier regions of the structure, together with subsequent retrapping, can be significant. Device engineering requires a full understanding of the kinetics of these electronic transitions. We have previously reported a study of the thermal quenching of the photoluminescence of $In_yGa_{1-y}As/GaAs$ and $In_yGaAs_{1-y}/Al_xGa_{1-x}As$ quantum-well structures.[2] At temperatures above 10–100 K, an Arrhenius behavior was observed, leading to strong quenching of the photoluminescence (PL) at 300 K, in agreement with previous authors.[3,4] We modeled this behavior using a simple rate-equation description in which each quantum well in a multiple-quantum-well (MQW) structure was treated separately and obtained reasonable agreement with the data for thermal activation energies close to the difference between the barrier band-gap energy and the PL emission energy. This showed that the mechanism of quenching was thermal emission of electron-hole pairs to the barriers rather than emission of carriers of either sign separately. In $In_yGa_{1-y}As/Al_xGa_{1-x}As$ MQW structures we found a much lower activation energy,[2] implying the presence of another nonradiative recombination channel, probably through defects introduced by the Al.[4]

In the present paper we report data on further structures containing $Al_xGa_{1-x}As$ and show that even at concentrations as low as 5% the Al-related nonradiative channel remains dominant, quenching the PL of $In_yGa_{1-y}As$ quantum wells adjacent to the $Al_xGa_{1-x}As$ layers. This nonradiative channel is not observed in samples with a spacer layer of GaAs separating the $In_yGa_{1-y}As$ and the $Al_xGa_{1-x}As$. We present also a more detailed theoretical analysis of multiple-quantum-well samples in which we include interactions between the wells in a MQW, and thereby reproduce some small features of the experimental data not explained by the simple model of Ref. 2. Applied to MQW samples, the coupled-well model has fewer free-fitting parameters than the single-well model and yet fits the data with activation energies which are exactly the difference between the barrier band-gap energy and the photoluminescence energy. We introduce temperature dependence into the radiative and trapping rates, and this yields physically reasonable values for the rates.

The similarity of all the fits and the good agreement with experiment shows that many parameters, such as the band offset ratio, and effects, such as retrapping, have little or no influence on the temperature dependence of the PL in multiple-quantum-well structures.

II. THEORETICAL MODEL

We model a multiple-quantum-well structure under optical excitation by the rate-equation scheme shown in Fig. 1, in which the barrier regions of the structure contain a single population n of electron-hole pairs and each of the w quantum wells contains an independent population m_i. With a pump or excitation rate P into the barrier region, and trapping and detrapping rate constants into each well of U_i and $U_i\beta_i$, where

$$\beta_i = \exp\left[-\frac{E_i}{kT}\right] \tag{1}$$

0163-1829/93/48(4)/2412(6)/$06.00

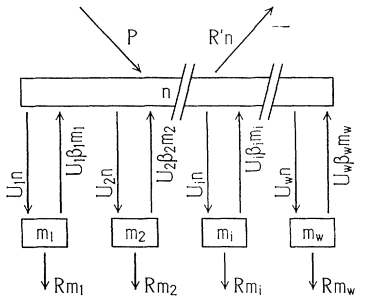

FIG. 1. Schematic diagram of the rate-equation model. The upper box represents the barrier band edge and the lower boxes are the quantum wells; n and m_i are the populations of electron-hole pairs in the levels. The transitions appearing in Eqs. (2) and (3) are marked. P is the pump or excitation rate, R and R' are the radiative and nonradiative recombination rates, assumed to be the same for all the wells, and U_i are the capture rates into the wells. The quantities β_i are the Boltzmann factors for each well, defined in Eq. (1).

and the E_i are the depths of the confined states below the barrier band edge, we assume a nonradiative recombination rate constant R' from the barrier and a radiative rate constant of R from the wells. We have used a constant R rather than different values R_i for each well for reasons discussed below, but for completeness we include R_i in the analysis. Then the rate equations describing the system in steady state are

$$\frac{dn}{dt}=0=P-R'n-\sum_{i=1}^{w}U_i n+\sum_{i=1}^{w}U_i\beta_i m_i\ , \tag{2}$$

$$\frac{dm_i}{dt}=0=U_i n-(U_i\beta_i+R_i)m_i\ . \tag{3}$$

Rearranging,

$$m_i=\frac{U_i n}{U_i\beta+R_i}$$

so that

$$n=P\frac{1}{R'+\sum_{1}^{w}\dfrac{U_i R_i}{U_i\beta_i+R_i}}$$

and the PL intensity from each well I_i is given by

$$I_i=R_i m_i=P\frac{R_i}{\left[\beta_i+\dfrac{R_i}{U_i}\right]\left[R'+\sum_{j=1}^{w}\dfrac{R_j}{\beta_j+\dfrac{R_j}{U_j}}\right]}\ . \tag{4}$$

Good fits to experiment can be obtained using Eq. (4), although the model omits several phenomena that might be thought to be relevant. Nonradiative recombination in the wells would decrease the intensity of the PL at all temperatures, but would not be detectable without a measurement of the absolute quantum efficiency of the PL. So R may contain a nonradiative component, but this will not affect a fit to experiment. Similarly, some part of R' might be radiative, but this will not affect the QW intensities I_i. Excitons will be formed at low temperature and their thermal ionization may enter into the temperature dependence of R. Most surprisingly, as we noted in Ref. 2, we do not need to write Eq. (1) separately for electrons and holes, with a β_e and a β_h, and so the band offset ratio appears to be irrelevant to the temperature dependence of QW photoluminescence.

The temperature dependence of Eq. (4) is dominated by the exponential in β and the fit to experiment gives the activation energies E_i and the relative rates. However, we have fitted the data (see below) under two assumptions to test whether further information on the physics of quantum wells can in fact be derived from these experiments. First, as in Ref. 2, we have fitted the data under the assumption that all the rates are independent of temperature (apart from terms in β). However, the radiative rates are expected to decrease with temperature over a large part of the range of these experiments, from the calculations of Haug,[5] as

$$R=\frac{R_0}{T}\ .$$

Similarly, U and R' are expected to increase with temperature. For simplicity, we assume a linear dependence for them, $U\propto R'\propto T$. Since the PL intensity depends only on the relative values of these rates, R, U, and R',[2] we may then include all the temperature dependence in R and so we have carried out a second fit to the data using a different R_0 and

$$R=\frac{R_0}{T^2}\ . \tag{5}$$

The data can be fitted equally well either with constant R or with R given by Eq. (5). The temperature-dependent R gives a fit with more reasonable parameter values, as might be expected. It gives activation energies which are rather lower than those from the constant R fits and values of U which are several orders of magnitude smaller. Given the wide range in R implied by these two fits, we have not considered it worthwhile to include a well-width dependence of R —that is, to use R_i —as the radiative component of R is expected to vary by only a factor of 2 or so over the range of well width used here,[6] and the well-width dependence of any nonradiative component of R is unknown. Obviously, if the lifetimes were to be measured in the same sample as a function of temperature using picosecond time-resolved spectroscopy, the experimental values should be used instead of Eq. (5). Feldmann *et al.*[7] have reported the temperature dependence of the lifetime of PL in $Al_xGa_{1-x}As/GaAs$ quantum wells up to 40 K and find a nearly linear increase with temperature from 1 ns at 4 K.

The value of R (or of R_0) depends on the physics of radiative recombination. At low temperature, it is about 1 GHz, corresponding to the well-established quantum-well exciton lifetime of about a nanosecond.[6,7] At higher temperatures, it is less clear what value to expect and we return to this question below (Sec. II B). The trapping time

U^{-1} is expected to be not dissimilar to hot carrier thermalization times which are a few picoseconds. Diffusion of carriers to the quantum wells is not considered in the model, although it does enter into observations of the PL rise time (typically 100 ps). The nonradiative rate R' is related to the quantum efficiency of luminescence at low temperature, and for this to be significantly less than unity R' must be of the same order of magnitude as ΣU. We take it as equal throughout our calculations.

It is worth noting that none of the parameters affect the sharpness of the elbow between the Arrhenius straight line at high temperature and the saturated intensity at low temperature. Consequently, if the data show a more rounded elbow, further physical effects than those considered here must be invoked (see Sec. II A).

In fitting a single quantum well, there are some tradeoffs so that the rate constants are not uniquely determined. A small change in E_A can be largely compensated by a change in U, to keep the elbow of the quenching curve at the same temperature. The vertical position of the curve, which depends on U/R', can then be restored by changing P. In contrast, in the coupled-well model, all wells have the same P and so the values of U_i are determined by the low-temperature intensities. Then only E_A is available to fit both the temperature of the elbow and the slope of the Arrhenius quenching. A successful fit is thus a more stringent test of the coupled-well model than it is for the single-well model. The ability of the model to fit the MQW data with parameter values not very different from these predictions indicates that we have not omitted any significant relevant physics from the problem.

III. EXPERIMENTAL DETAILS AND RESULTS

The five samples we studied are listed in Table I. They were grown by molecular-beam epitaxy in a VG V80H reactor using solid sources. The substrate temperature was 530 °C and the GaAs growth rate was 1 monolayer per second. All the samples were nominally undoped. Three samples were $In_yGa_{1-y}As/Al_xGa_{1-x}As$ single-quantum-well structures (SQW's) with varying Al contents in the barriers. One sample contained four $In_yGa_{1-y}As$ quantum wells in GaAs barriers (the data from this sample were reported in Ref. 2). Finally, a sample was grown containing two $GaAs/Al_xGa_{1-x}As$ classical wells, 1500 Å thick; one of these classical wells contained three quantum wells of different $In_yGa_{1-y}As$ compositions. The purpose of this sample was to test the effect of providing extra confinement to the $In_yGa_{1-y}As$ quantum wells but without direct contact between the $Al_xGa_{1-x}As$ and the $In_yGa_{1-x}As$ layers. The GaAs classical well, No. 1 in Table I, was provided for a comparative measurement of the thermal quenching in GaAs with $Al_xGa_{1-x}As$ barriers to prevent surface recombination.

Photoluminescence experiments were carried out in a helium flow cryostat. Argon laser radiation at 514 nm was used for excitation, at a power density of about 10 W cm^{-2}. Because there can be significant temperature lags between the cryostat temperature sensor and the sample, a second sensor was provided on the sample mount. Spectra were recorded only when the two temperature sensors agreed. The spectra were corrected for the response of the spectrometer and detector and the peaks for each quantum well were integrated numerically, so that changes in PL linewidth with temperature would not matter. We consider the $In_yGa_{1-y}As/Al_xGa_{1-x}As$ SQW structures first, to establish the effect of the temperature-dependent R, and then present the fits to the MQW samples.

A. $In_yGa_{1-y}As/Al_xGa_{1-x}As$ SQW structures

The results from these samples are plotted in Fig. 2, together with theoretical fits to the data using Eq. (4) with $w=1$. The parameters used for the fits are given in Table II. Note that the fits with constant R (dotted lines) and with a T^{-2} dependence (solid lines) are almost indistinguishable over the range of intensities observed experimentally.

TABLE I. Sample parameters. In the MQW samples, the wells are listed in order down from the free surface of the structure.

Sample	Barriers	Wells	PL energy at 10 K (eV)
ME739	$Al_{0.05}Ga_{0.95}As$	1: 100 Å $In_{0.20}Ga_{0.80}As$	1.348
ME746	$Al_{0.10}Ga_{0.90}As$	1: 100 Å $In_{0.20}Ga_{0.80}As$	1.349
ME741	$Al_{0.20}Ga_{0.80}As$	1: 100 Å $In_{0.20}Ga_{0.80}As$	1.347
ME501	500 Å GaAs	1: 120 Å $In_{0.20}Ga_{0.80}As$	1.349
		2: 60 Å $In_{0.20}Ga_{0.80}As$	1.405
		3: 40 Å $In_{0.20}Ga_{0.80}As$	1.437
		4: 30 Å $In_{0.20}Ga_{0.80}As$	1.465
ME614	200 Å $Al_{0.2}Ga_{0.8}As$	1: 1500 Å GaAs	1.514
		2: 1500 Å GaAs containing:	
		2(a): 100 Å $In_{0.25}Ga_{0.75}As$	1.299
		2(b): 100 Å $In_{0.17}Ga_{0.83}As$	1.381
		2(c): 100 Å $In_{0.10}Ga_{0.90}As$	1.443

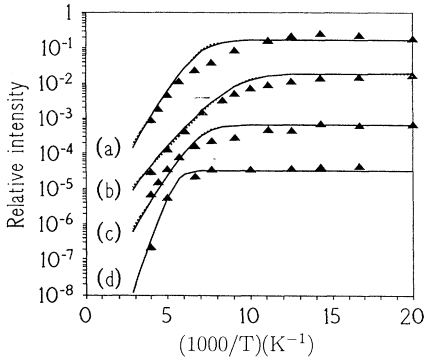

FIG. 2. Data for the three $In_{0.20}Ga_{0.80}As/Al_xGa_{1-x}As$ SQW samples are shown, together with the theoretical fits from Eq. (4) with $w=1$, using both a constant R (dotted lines) and $R \propto T^{-2}$. Data points and curves are for (a) $Al_{0.05}Ga_{0.95}As$, (b) $Al_{0.10}Ga_{0.90}As$ well, and (c) $Al_{0.20}Ga_{0.80}As$ barriers. Finally, the data and solid curve (d) are for the GaAs luminescence from the 1500-Å classical wells in $Al_{0.20}Ga_{0.80}As$ barriers in sample ME614.

The results are qualitatively the same as the $In_yGa_{1-y}As/Al_xGa_{1-x}As$ MQW sample reported previously[2] in that the activation energy shows no systematic variation with well depth or PL energy; also the sum of the PL energy and the activation energy is much less than the barrier band gaps. With a constant R, the prefactor (U/R) is within the range observed previously ($10^{4.2}$–$10^{5.3}$). From these samples it is clear that an Al-related nonradiative recombination mechanism is still dominant even at the modest Al content of 5%. Unlike the three wells in the previously reported MQW, these wells show a deviation from the theoretical fit in the region of the elbow; this would normally indicate a broad range of radiative or nonradiative rates so that the experimental curve is an average of a distribution of curves shifted on the horizontal axis.[8] In $In_yGa_{1-y}As/Al_xGa_{1-x}As$ quantum wells such an explanation seems unlikely. More probable is that there are several defect-related nonradiative mechanisms, in $Al_xGa_{1-x}As$. We may be observing here the same process as reported by Toyada, Tomita, and Hanba[9] in bulk $Al_xGa_{1-x}As$, leading to thermal quenching from 40 K with an activation energy of 32 meV, in addition to the mechanism in the sample of Ref. 2. At all events, there is plainly considerable scatter in the thermal quenching of $In_yGa_{1-y}As/Al_xGa_{1-x}As$ samples, as might be expected for defects related to growth conditions; this offers some prospect that growth optimization could reduce or eliminate the Al-related nonradiative recombination.

The fits to the data using the temperature-dependent R of Eq. (5) are almost indistinguishable from the constant R fits. Accordingly, these data cannot reveal the real temperature dependence of the rate constants—any power law in T could be used, from $T^{<0}$ to $T^{>2}$. However, it should be noted that the temperature-dependent R gives activation energies E_A that are significantly lower, and the capture rates U are orders of magnitude smaller. A reasonable value for R at low temperature is about 1 GHz (radiative lifetime of 1 ns) and in the constant R fit this gives 10^{14} Hz for U and R'. These are higher than the highest typical phonon frequencies of 10^{13} Hz. On the other hand, using Eq. (5), a reasonable value for R_0 is 10^{11} Hz K^2 (giving a 1-ns lifetime at 10 K) and the fits using this value correspond to $U=5\times10^{10}$ Hz at low temperature, which is much more plausible.

B. $In_yGa_{1-y}As/Al_xGa_{1-x}As$ MQW samples

First of all, we have refitted the data from the $In_yGa_{1-y}As/GaAs$ MW sample, ME501, reported in Ref. 2. We use the coupled wells model of Eq. (4) instead of the single-well model of Ref. 2, and fit with both the constant R and the temperature-dependent R. Results are shown in Fig. 3 and the parameter values are given in Table II. The values for constant R differ somewhat from those in Ref. 2, but the sums of the activation energies and the PL energies are still consistently above the GaAs band gap (1.519 14 eV) by up to 20 meV. However, the fits now account for the increases in the intensities of the deeper wells when a shallower well begins to quench.

TABLE II. Fitting parameters.

Sample and quantum well	Constant radiative rate $R=1$ E_A (meV)	U/R	$E_{PL}+E_A$ (eV)	Temperature-dependent radiative rate $R=100T^{-2}$ E_A (meV)	U/R	$E_{PL}+E_A$ (eV)
ME739	140	10^5	1.488	105	50	1.453
ME746	100	10^5	1.449	70	40	1.419
ME741	140	10^5	1.487	105	50	1.452
ME501 No. 1	190	1.2×10^8	1.539	170	9.5×10^4	1.519
ME501 No. 2	130	10^8	1.540	114	8×10^4	1.519
ME501 No. 3	85	1.8×10^7	1.522	82	1.4×10^4	1.519
ME501 No. 4	75	2.5×10^7	1.548	54	2×10^4	1.519
ME614 No. 1				220	5×10^3	1.724
ME614 No. 2(a)	300	3×10^7	1.599	260	8×10^4	1.559
ME614 No. 2(b)	145	10^7	1.526	138	2.5×10^4	1.519
ME614 No. 2(c)	75	1.2×10^7	1.521	63	3.2×10^4	1.509

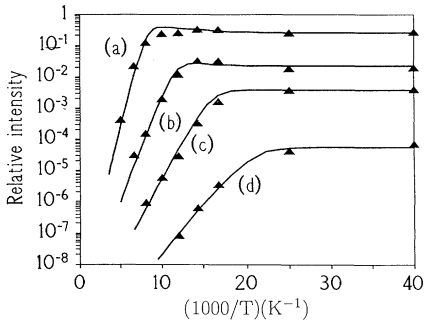

FIG. 3. Data for the $In_yGa_{1-y}As/GaAs$ 4QW sample are shown together with the theoretical fits from Eq. (4) with $w=4$, using $R \propto T^{-2}$. Data points and curves are for (a) the 120-Å well, (b) the 60-Å well, (c) the 40-Å well, and (d) the 30-Å well.

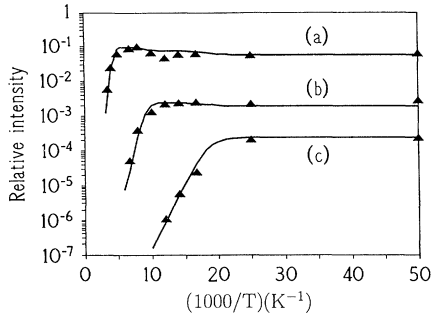

FIG. 4. Data for the $In_yGa_{1-y}As/GaAs/Al_xGa_{1-x}As$ MQW sample are shown together with the theoretical fits from Eq. (4) with $w=3$, using $R \propto T^{-2}$. Data points and curves are for (a) the $In_{0.25}Ga_{0.75}As$ well, (b) the $In_{0.17}Ga_{0.83}As$ well, and (c) the $In_{0.10}Ga_{0.90}As$ well.

This effect is due to retrapping of some of the thermally detrapped carriers. The values of U_i are again around $10^{7.5}R$, which for a constant R with a low-temperature value of 1 GHz gives over 10^{16} Hz for U_i. This is so far above phonon frequencies as to be unphysical.

With the temperature-dependent R, it is possible to fit the data satisfactorily with activation energies which sum with the low-temperature PL energies to equal the low-temperature GaAs barrier band gap precisely; these fits are shown in Fig. 3. The values of U_i are also more reasonable than those obtained with the constant R. If R is taken to be about 1 GHz at 10 K and to decrease with T according to Eq. (5) at higher temperatures, then the values of U_i of 10^4-10^5 correspond to rates of $10^{13}-10^{14}$ Hz, or subpicosecond trapping times. This is a little too fast, but much more reasonable than the values from the constant R fit. However, this may be to overestimate the value of R at elevated temperature. The temperature dependence of the carrier lifetime is now well established. Radiative recombination at room temperature is expected to be bimolecular,[5] so that

$$I_{\mathrm{PL}} \approx Bn^2 L_z \ ,$$

where n is the carrier density and L_z is the quantum-well width. Typical values for B are around 10^{-10} cm^3 s^{-1}, so that taking $L_z=100$ Å and the excitation power as 10 W cm^{-2} we have a carrier density of $n=10^{18}$ cm^{-3} in the quantum wells or 10^{12} cm^{-2} as a sheet carrier density. This implies an average carrier lifetime (defined as sheet density, 10^{12} cm^{-2}, over creation rate, $\sim 10^{20}$ cm^{-2}) of about 10 ns, not very different from the low-temperature value. But when the PL intensity is thermally quenched by four orders of magnitude, the carrier density becomes 10^{10} cm^{-2} and the lifetime rises to 1 μs. In our model, this gives values around $10^{10}-10^{11}$ Hz for U (from Table II), consistent with the trapping times of the order of 100 ps observed by time-resolved spectroscopy.[6]

The data and the theoretical fit for the $In_yGa_{1-y}As/GaAs/Al_xGa_{1-x}As$ sample ME614 are shown in Fig. 4. The model predicts accurately the quenching of the three $In_yGa_{1-y}As$ wells, together with the increases in intensity due to retrapping. Here, however, only the middle well can be fitted with an activation energy precisely equal to the depth of the emitting state below the barrier. There is a 10 meV discrepancy for the shallowest well (which we attribute to experimental error) and a large discrepancy of 40 meV for the deepest well. On the other hand, the GaAs classical well does satisfy $E_{\mathrm{PL}}+E_A=E_g^{\mathrm{barrier}}$ to within experimental error, using[10]

$$E_g(x)=1.519+1.087x+0.438x^2$$

for the band gap of $Al_xGa_{1-x}As$ and taking $x=0.18$ (which is within the probable range of composition for molecular-beam epitaxy growth of, nominally, $Al_{0.2}Ga_{0.8}As$).

The emission which we attribute to the classical well No. 1 in this sample is of course also due to the classical well No. 2 containing the quantum wells. It will also be due to other layers of GaAs in the sample, the buffer layer and the cap. However, PL from the cap is suppressed by surface recombination, and PL from the buffer is suppressed by carrier diffusion into the substrate. At high temperature, when the $In_yGa_{1-y}As$ quantum-well emission is largely quenched, we expect the well No. 2 to give the same PL as well No. 1, with the same temperature dependence. Since this quenches very close to the quenching of the deepest $In_yGa_{1-y}As$ well, it is probable that its temperature dependence has been exaggerated by the simultaneous loss of carriers from the GaAs, and this is responsible for its activation energy appearing to be 40 meV too high.

It is clear from the temperature dependence of the GaAs emission that the Al-related loss mechanism seen in the $In_yGa_{1-y}As/Al_xGa_{1-x}As$ SQW samples affects neither the GaAs classical wells nor the $In_yGa_{1-y}As$ quantum wells, although the outer two are separated from the $Al_xGa_{1-x}As$ layers by only 150 Å of GaAs. This is consistent with the attribution of the loss mechanism to a defect in the $Al_xGa_{1-x}As$, since in neither the classical wells nor the quantum wells does much of the wave function extend into the $Al_xGa_{1-x}As$ barriers—certainly, much less of the wave function than in the $In_yGa_{1-y}As/Al_xGa_{1-x}As$ SQW's.

IV. CONCLUSIONS

We have shown that the photoluminescence of both $In_yGa_{1-y}As/GaAs$ multiple quantum wells and $GaAs/Al_xGa_{1-x}As$ classical wells can be fitted by a rate-equation model in which the mechanism of thermal quenching is emission to the barrier. Coupling between the wells is included and accounts for small deviations in the PL intensity from a single-well model. In MQW structures, there is essentially only one free-fitting parameter per well, U/R, and the fit yields physically reasonable parameter values.

This is quite surprising. Several physical effects have been omitted from the model, notably carrier diffusion rates, but also accurate temperature dependences of the various rate constants. Nevertheless, the activation energies are close to those predicted by the model and this confirms its validity. The completely different rates and activation energies observed in the $In_yGa_{1-y}As/Al_xGa_{1-x}As$ samples then clearly reveal a different nonradiative loss mechanism.

*Present address: Network Fibres Ltd., Lancaster House, Farnborough Business Centre, Eelmoor Road, Farnborough, Hants GU14 7QN, England.

[1]R. W. Lucky, IEEE Spectrum **29**, 6 (March, 1992).

[2]J. D. Lambkin, D. J. Dunstan, K. P. Homewood, and L. K. Howard, Appl. Phys. Lett. **57**, 1986 (1990).

[3]R. L. S. Devine, Semicond. Sci. Technol. **3**, 1171 (1988).

[4]P. B. Kirby, M. B. Simpson, J. D. Wilcox, R. S. Smith, T. M. Kerr, B. A. Miller, and C. E. C. Wood, Appl. Phys. Lett. **53**, 2158 (1988).

[5]A. Haug, Appl. Phys. B **44**, 151 (1987).

[6]Th. Amand, X. Marie, B. Dareys, J. Barrau, M. Brousseau, D. J. Dunstan, J. Y. Emery, and L. Goldstein, J. Appl. Phys. **72**, 2077 (1992).

[7]J. Feldmann, G. Peter, E. O. Göbel, P. Dawson, K. Moore, C. Foxon, and R. J. Elliot, Phys. Rev. Lett. **59**, 2337 (1987).

[8]D. J. Dunstan and F. Boulitrop, J. Phys. (Paris) Colloq. **42**, C4-331 (1981).

[9]T. Toyada, M. Tomita, and S. Hanba, Semicond. Sci. Technol. **1**, 295 (1986).

[10]*Data in Science and Technology: Semiconductors,* edited by O. Madelung (Springer-Verlag, Berlin, 1991).